Available online at www.sciencedirect.com
ScienceDirect
Journal of the European Ceramic Society 30 (2010) 1483–1488
www.elsevier.com/locate/jeurceramsoc

Fabrication and thermal expansion properties of $ZrW_2O_8/Zr_2WP_2O_{12}$ composites

Jun-ichi Tani *, Masanari Takahashi, Hiroyasu Kido

Department of Electronic Materials, Osaka Municipal Technical Research Institute, 1-6-50 Morinomiya, Joto-ku, Osaka 536-8553, Japan

Received 23 July 2009; received in revised form 29 October 2009; accepted 17 November 2009
Available online 31 December 2009

Abstract

$ZrW_2O_8/Zr_2WP_2O_{12}$ composites were fabricated by sintering ZrW_2O_8–$Zr_2WP_2O_{12}$ powder mixtures at 1473 K for 1 h, and their negative thermal expansion properties were investigated. The relative density of sintered pure-phase ZrW_2O_8 was 72.3%, while that of the sintered composites was 88.4–92.3%. In the composites, the observed hysteresis in the thermal expansion data was small because of the small difference between the CTEs of ZrW_2O_8 and $Zr_2WP_2O_{12}$. The CTE of the composites was negative and increased with the $Zr_2WP_2O_{12}$ content. When the $Zr_2WP_2O_{12}$ volume fraction in the composites was increased from 0 to 75 vol%, the CTEs of the composites increased from -9.1×10^{-6} to $-3.1 \times 10^{-6}\,K^{-1}$ and from -5.0×10^{-6} to $-1.9 \times 10^{-6}\,K^{-1}$ over the temperature ranges of 323–373 and 473–673 K, respectively. In composites with $Zr_2WP_2O_{12}$ volume fractions of 0–25 vol%, the experimentally obtained CTE values were in good agreement with the calculated values obtained by assuming mixed law behavior.

Keywords: Sintering; Composites; Thermal expansion; ZrW_2O_8

1. Introduction

Zirconium tungstate (ZrW_2O_8) exhibits a relatively large isotropic negative thermal expansion over a wide temperature range of 0.3–1050 K.[1,2] Therefore, ZrW_2O_8 is considered an attractive candidate for use as a filler material to control the coefficient of thermal expansion (CTE) of ceramics, glasses, metals, and polymers. Recent studies have reported the successful fabrication of ZrW_2O_8 composites, e.g., ZrO_2/ZrW_2O_8,[3–5] SnO_2/ZrW_2O_8,[6] SiO_2/ZrW_2O_8,[7] $ZrW_2O_8/Zr_2WP_2O_{12}$,[8] low-melting glass/ZrW_2O_8,[9] Cu/ZrW_2O_8,[10–12] Al/ZrW_2O_8,[13] polyester/ZrW_2O_8,[14] epoxy/ZrW_2O_8,[14] polyimide/ZrW_2O_8,[15] and phenolic resin/ZrW_2O_8[16] systems. A decrease in the CTE values of these composites has been observed when the amount of ZrW_2O_8 filler is increased. However, the thermal expansion behavior of the composites is complicated. ZrW_2O_8 has two cubic phases at ambient pressure (α-phase below 423 K and β-phase above 423 K) and one orthorhombic phase at high pressures (γ-phase). The CTEs of these three phases are negative but vary in magnitude, with $CTE_\alpha = -8.7 \times 10^{-6}\,K^{-1}$, $CTE_\beta = -4.9 \times 10^{-6}\,K^{-1}$, and $CTE_\gamma = -1.0 \times 10^{-6}\,K^{-1}$.[1,2,17] Some of the composites show unusually large hysteresis in thermal expansion because of the stress-induced formation of γ-ZrW_2O_8, which could pose a problem in practical applications.[3,5] When the thermal expansion mismatch between the matrix and filler is small, the formation of γ-ZrW_2O_8 is inhibited. Therefore, for realizing practical applications, it is desirable to develop composites of ZrW_2O_8 and negative/low thermal expansion materials. Evans et al.[18] and Mary and Sleight[19] reported that $Zr_2(WO_4)(PO_4)_2$ (also referred to as $Zr_2WP_2O_{12}$) showed negative thermal expansion. Recently, Isobe et al.[8] reported the liquid phase sintering of $ZrW_2O_8/Zr_2WP_2O_{12}$ composites (with a P_2O_5 content of less than 40%) using ZrO_2–WO_3–$NH_4H_2PO_4$ powder mixtures. The relative density of their samples, which contained >5 mol% P_2O_5, was about 90%. The identified phases were mainly ZrW_2O_8 with small amounts of WO_3, ZrO_2, and $Zr_2WP_2O_{12}$.

In this study, we present a new fabrication route whereby $ZrW_2O_8/Zr_2WP_2O_{12}$ composites can be obtained over the entire range of possible $Zr_2WP_2O_{12}$ volume fractions, i.e., 0–100 vol%, by sintering ZrW_2O_8–$Zr_2WP_2O_{12}$ powder mix-

* Corresponding author. Tel.: +81 6 6963 8081; fax: +81 6 6963 8099.
E-mail address: tani@omtri.or.jp (J.-i. Tani).

0955-2219/$ – see front matter © 2009 Elsevier Ltd. All rights reserved.
doi:10.1016/j.jeurceramsoc.2009.11.010

tures. The composition dependence of the thermal expansion of the composites was investigated in detail.

2. Experimental procedure

ZrW_2O_8 was prepared from two commercially available precursor materials: zirconium oxychloride octahydrate ($ZrCl_2O{\cdot}8H_2O$; Wako Pure Chemical Industries Ltd., Osaka, Japan) and ammonium tungstate para pentahydrate ($(NH_4)_{10}W_{12}O_{41}{\cdot}5H_2O$; Wako Pure Chemical Industries Ltd.). Stoichiometric mixtures of the precursors were aged in a water bath and stirred with a magnetic stirrer at 373 K for 3 h; the mixtures were then dried. To avoid the problem of high weight loss due to inorganic precursor decomposition, a separate burnout step was performed at 873 K for 3 h before pressing and firing so that a large volume of the volatile species could be eliminated. Powder mixtures weighing 10 g were pressed at 60 MPa into pellets (30 mm in diameter) using a hand press and then fired in air to 1473 K (heating rate: 20 K/min) with a dwell time of 3 h in a Pt crucible. The heated pellets were then rapidly quenched in liquid nitrogen. The pellets were ground to a powder by wet milling in ethanol for 24 h. The mean volume particle size, as determined by laser diffraction and a scattering method (model LA-920, Horiba Ltd., Kyoto, Japan), was 3.2 μm. Phase analysis was carried out by X-ray powder diffraction (XRD; model RINT 2500, Rigaku, Tokyo, Japan), which utilized CuK_α radiation at 40 kV and 50 mA; the analysis revealed that the powder had a phase-pure cubic α-phase structure. Commercially available $Zr_2WP_2O_{12}$ powder (KCM Corporation, Nagoya, Japan) was used, and the mean volume particle size was 0.94 μm. ZrW_2O_8 and $Zr_2WP_2O_{12}$ powders were mixed together using an agate mortar and pestle and were pressed into bars (5 mm × 5 mm × 20 mm) at 60 MPa using a hand press. The composites were prepared by firing in air at 1473 K (heating rate: 20 K/min) with a dwell time of 1 h in a Pt crucible. The heated pellets were then rapidly quenched in liquid nitrogen.

The thermal expansion of the bars was measured using a thermal mechanical analyzer (model TMA 8310, Rigaku, Tokyo, Japan) in N_2 flowing at 50 ml/min with a heating rate of 5 K/min over the temperature range of 300–680 K. The CTE was determined from the slope of the plot between the thermal expansion and the temperature over two temperature ranges: 323–373 and 473–673 K. The microstructures of the composites were observed with a scanning electron microscope and energy dispersive X-ray spectrometer (SEM-EDX; model JSM-6460LA, JEOL, Tokyo, Japan) at 20 kV and a working distance of 10 mm. Phase analysis was carried out by XRD, which utilized CuK_α radiation at 40 kV and 50 mA. Phase identification was accomplished by comparing the experimental XRD patterns with the standards compiled by the International Center for Diffraction Data (ICDD, Newtown Square, PA).

3. Results and discussion

The XRD patterns of the composites (Fig. 1) revealed the presence of γ-ZrW_2O_8, $Zr_2WP_2O_{12}$, and γ-ZrW_2O_8.

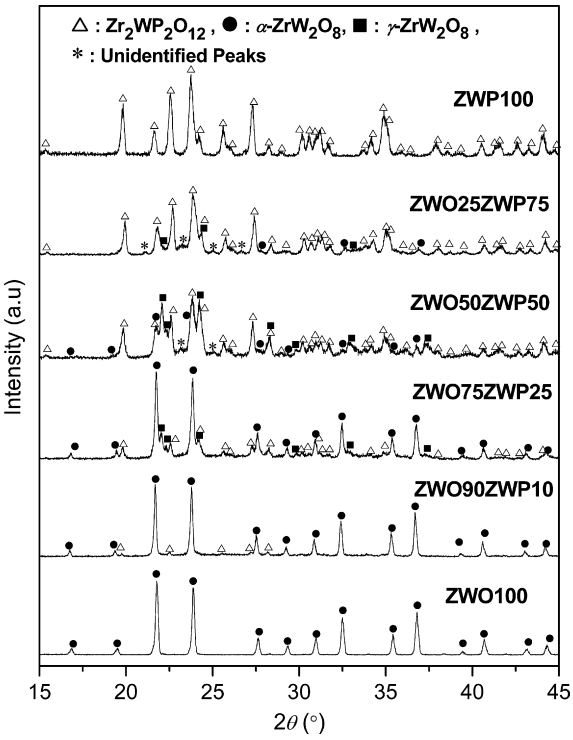

Fig. 1. XRD patterns of the composites obtained by sintering ZrW_2O_8–$Zr_2(WO_4)(PO_4)_2$ powder mixtures in air at 1473 K for 1 h.

Furthermore, the XRD patterns of composites containing 75 vol% $Zr_2WP_2O_{12}$ (ZWO25ZWP75) and 50 vol% $Zr_2WP_2O_{12}$ (ZWO50ZWP50) showed small unidentified peaks.

The relative density of sintered pure-phase ZrW_2O_8 was 72.3%, while that of the sintered ZrW_2O_8/$Zr_2WP_2O_{12}$ composites were 88.4–92.3% (Fig. 2). Thus, the $Zr_2WP_2O_{12}$ phase effectively facilitated the densification of ZrW_2O_8. The relative densities of our composites were in good agreement with the corresponding value (about 90%) reported by Isobe et al., who pointed out that $Zr_2WP_2O_{12}$ cannot function as the liquid phase since its melting point is >2023 K.[20] They considered

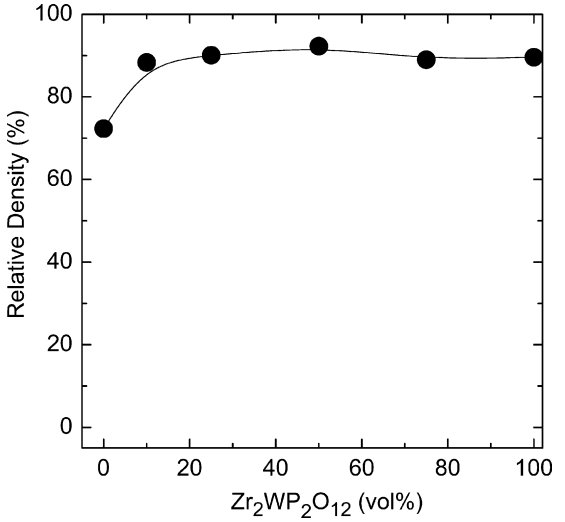

Fig. 2. Relative density of the ZrW_2O_8/$Zr_2WP_2O_{12}$ composites.

that a ZrO_2–P_2O_5 liquid phase was formed during the initial and/or intermediate stage of sintering and that this phase filled the gaps between the ZrW_2O_8 grains. In our process, however, the addition of $Zr_2WP_2O_{12}$ resulted in a high relative density. $Zr_2WP_2O_{12}$ is easier to sinter than ZrW_2O_8. The relative density of sintered pure-phase $Zr_2WP_2O_{12}$ was 89.6%, which is much higher than that of ZrW_2O_8 (72.3%). Moreover, we consider that the addition of small $Zr_2WP_2O_{12}$ particles increases the packing efficiency because the mean volume particle size of the precursor $Zr_2WP_2O_{12}$ powder was 0.94 μm, which is much smaller than that of ZrW_2O_8 (3.2 μm).

SEM backscattered electron images of the polished surface of the ZrW_2O_8/$Zr_2WP_2O_{12}$ composites revealed the presence of numerous large pores in the microstructure of pure-phase ZrW_2O_8 (Fig. 3(a)); this observation correlates with the fact that the relative density of sintered ZrW_2O_8 is 72.3%. EDX analysis revealed that the small black grains and large white/gray grains in the composites were $Zr_2WP_2O_{12}$ and ZrW_2O_8, respectively (Fig. 3(b)–(e)). The grain size of ZrW_2O_8 was larger than that of $Zr_2WP_2O_{12}$, because the mean volume particle size of the precursor powder for ZrW_2O_8 was larger than that for $Zr_2WP_2O_{12}$. The images of pure-phase ZrW_2O_8 and $Zr_2WP_2O_{12}$ indicated areas of different contrast. The light gray areas were ZrW_2O_8/$Zr_2WP_2O_{12}$ grains whereas the dark gray areas were pores (Fig. 3(a) and (f)). In comparison with pure-phase ZrW_2O_8, sintered pure-phase $Zr_2WP_2O_{12}$ was dense and

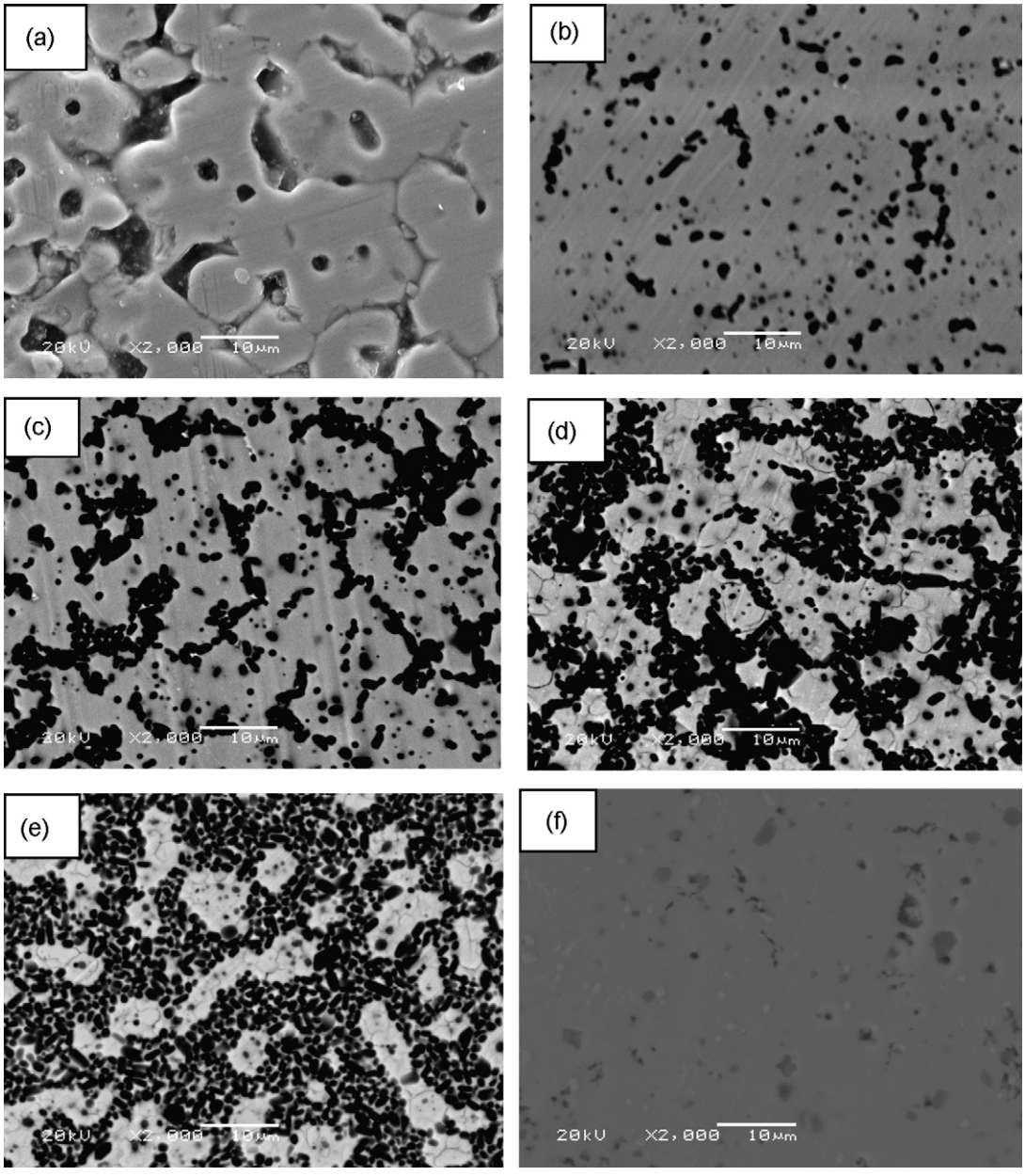

Fig. 3. SEM backscattered electron images of the polished surfaces of the ZrW_2O_8/$Zr_2WP_2O_{12}$ composites at the following $Zr_2WP_2O_{12}$ volume fractions: (a) 0 vol%, (b) 10 vol%, (c) 25 vol%, (d) 50 vol%, (e) 75 vol%, and (f) 100 vol%.

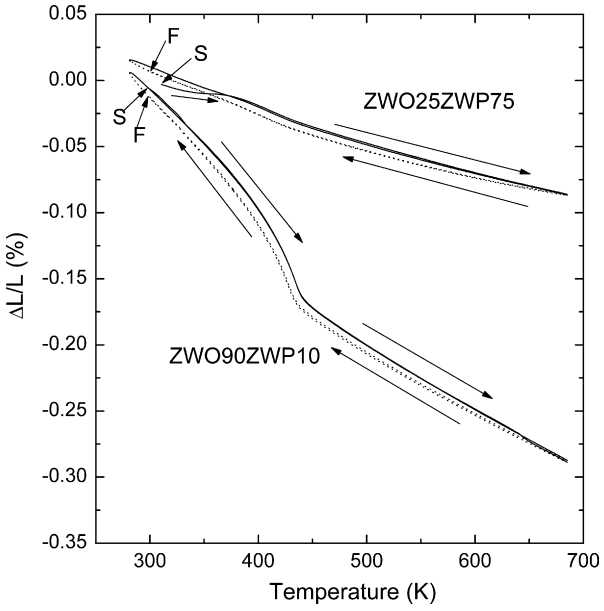

Fig. 4. Thermal expansion behavior of $ZrW_2O_8/Zr_2WP_2O_{12}$ composites with 10 and 75 vol% $Zr_2WP_2O_{12}$ during two thermal cycles. Start and finish are marked by "S" and "F," respectively. The solid and dotted lines indicate the results for the heating and cooling measurements, respectively.

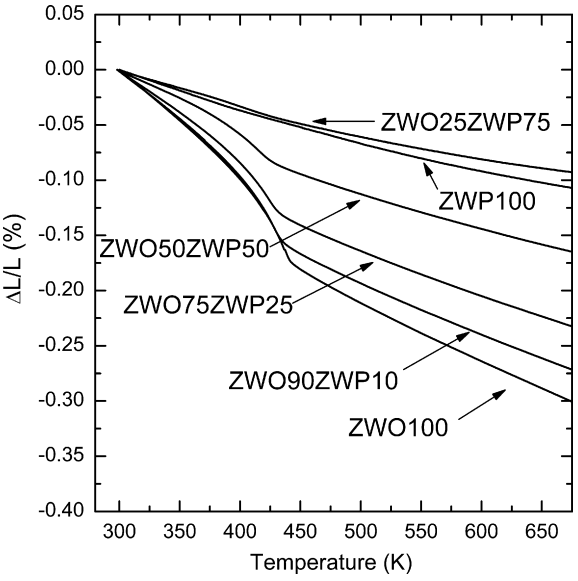

Fig. 5. Thermal expansion of the $ZrW_2O_8/Zr_2WP_2O_{12}$ composites based on initial cooling measurements after heating.

its microstructure showed only a few small pores (Fig. 3(f)); this is because the relative density of sintered pure-phase $Zr_2WP_2O_{12}$ is higher than that of pure-phase ZrW_2O_8.

We investigated the thermal expansion behavior of the $ZrW_2O_8/Zr_2WP_2O_{12}$ composites (ZWO25ZWP75 and ZrW_2O_8–10 vol% $Zr_2WP_2O_{12}$ (ZWO90ZWP10)) over two thermal cycles (Fig. 4). In the first heating scan for ZWO25ZWP75, we observed a slightly higher thermal expansion, along with a volume change, over the temperature range of 300–380 K; this observation can be attributed to $\gamma \rightarrow \alpha$ phase transformation, which occurs in conjunction with a volume change. In both ZWO25ZWP75 and ZWO90ZWP10, a small hysteresis was observed in the thermal expansion data between the heating and cooling measurements. For both ZWO25ZWP75 and ZWO90ZWP10, the second cycle was in good agreement with the first cycle, with the exception of the initial first heating scan for ZWO25ZWP75. In some composites, such as SnO_2/ZrW_2O_8,[6] low-melting glass/ZrW_2O_8,[9] and Cu/ZrW_2O_8,[10–12] an unusually large hysteresis in the thermal expansion data has been observed because of the stress-induced formation of γ-ZrW_2O_8. However, in our $ZrW_2O_8/Zr_2WP_2O_{12}$ composites, the observed hysteresis in the thermal expansion data was small. This result can be explained by the fact that the thermal expansions of both ZrW_2O_8 and $Zr_2WP_2O_{12}$ are negative and the CTE difference between ZrW_2O_8 and $Zr_2WP_2O_{12}$ is small.

Initial cooling measurements after heating revealed that the thermal expansion of the $ZrW_2O_8/Zr_2WP_2O_{12}$ composites decreased with temperature and increased with the $Zr_2WP_2O_{12}$ content (Fig. 5). The shape of the thermal expansion curve of the composites changed due to the phase transition between α-ZrW_2O_8 and β-ZrW_2O_8. The $\alpha \leftrightarrow \beta$ phase transition temperature (T_{trs}) of the composites decreased with an increase in the $Zr_2WP_2O_{12}$ content of the composites. At 0, 10, 25, 50, and 75 vol% $Zr_2WP_2O_{12}$, the composites showed T_{trs} values of 442, 434, 431, 427, and 422 K and their thermal expansions from 300 to 675 K were −0.30, −0.27, −0.23, −0.17, −0.09, and −0.11%, respectively. The CTEs of the composites were determined from the slopes of the experimental plots between thermal expansion and temperature over two temperature ranges: 323–373 and 473–673 K.

We plotted the experimentally obtained CTE values of the $ZrW_2O_8/Zr_2WP_2O_{12}$ composites as a function of the volume fraction of $Zr_2WP_2O_{12}$; for comparison, we calculated the CTE values of the composites by assuming the rule of mixtures (ROM)[21] and plotted these values on the same graph (Fig. 6).

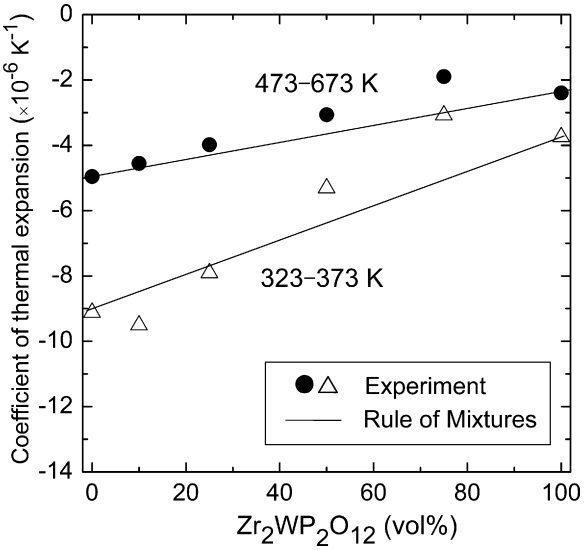

Fig. 6. Experimentally obtained CTE values and calculated CTE values (obtained by assuming the rule of mixtures (ROM)) of the $ZrW_2O_8/Zr_2WP_2O_{12}$ composites plotted as a function of the $Zr_2WP_2O_{12}$ volume fraction.

Over 323–373 and 473–673 K, the CTEs of ZrW_2O_8 were -9.1×10^{-6} and $-5.0 \times 10^{-6}\,K^{-1}$, while those of $Zr_2WP_2O_{12}$ were -3.7×10^{-6} and $-2.4 \times 10^{-6}\,K^{-1}$, respectively. The CTEs of the ZrW_2O_8 and $Zr_2WP_2O_{12}$ in this study were in good agreement with previous experimental results.[1,2,18,22,23] The CTEs of the composites were negative and increased with the $Zr_2WP_2O_{12}$ content. When the $Zr_2WP_2O_{12}$ volume fraction in the composites was increased from 0 to 75 vol%, the CTEs of the composites increased from -9.1×10^{-6} to $-3.1 \times 10^{-6}\,K^{-1}$ and from -5.0×10^{-6} to $-1.9 \times 10^{-6}\,K^{-1}$ over 323–373 and 473–673 K, respectively.

The ROM serves as the first-order approximation to the overall calculation of the CTE of the composites:

$$\alpha_C = \alpha_{ZWP}\phi + \alpha_{ZWO}(1 - \phi) \quad (1)$$

where α_C, α_{ZWP}, and α_{ZWO} denote the CTEs of the composites, $Zr_2WP_2O_{12}$, and ZrW_2O_8, respectively, and ϕ is the volume fraction of $Zr_2WP_2O_{12}$. In the composites containing 0–25 vol% $Zr_2WP_2O_{12}$, the experimental and calculated CTE values were in good agreement over both the 323–373 and 473–673 K ranges. However, at 50–75 vol% $Zr_2WP_2O_{12}$, the experimental CTE values were positioned higher than the calculated values. As discussed above, in XRD analyses, small unidentified peaks, as well as small peaks corresponding to the high-pressure γ-ZrW_2O_8 phase ($CTE_\gamma = -1.0 \times 10^{-6}$ K),[17] were detected for the ZWO25ZWP75 and ZWO50ZWP50 composites. Therefore, the CTEs of the $ZrW_2O_8/Zr_2WP_2O_{12}$ composites might be influenced by small amounts of the unidentified phases and also by the γ-ZrW_2O_8 phase, which is closely related to the internal stress in the composites. Another possible reason is that the ROM model does not account for the influence of voids/cracks, the mechanical properties of ZrW_2O_8 and $Zr_2WP_2O_{12}$ phases, and the interface factors. Balch et al.[24] reported that the CTEs of Al–matrix composites, reinforced with SiC particles or microcellular form, were influenced by a small proportion of voids in the matrix. Because the relative density of the sintered $ZrW_2O_8/Zr_2WP_2O_{12}$ composites was 88.4–92.3%, the presence of pores/voids might reflect as the higher experimental CTEs than the calculated values.

4. Conclusions

$ZrW_2O_8/Zr_2WP_2O_{12}$ composites were fabricated by sintering ZrW_2O_8–$Zr_2WP_2O_{12}$ powder mixtures at 1473 K for 1 h, and their negative thermal expansion properties were investigated. The relative density of sintered pure-phase ZrW_2O_8 was 72.3%, while that of the sintered composites was 88.4–92.3%. In the composites, the observed hysteresis in the thermal expansion data was small because of the small difference between the CTEs of ZrW_2O_8 and $Zr_2WP_2O_{12}$. The CTE of the composites was negative and increased with the $Zr_2WP_2O_{12}$ content. When the $Zr_2WP_2O_{12}$ volume fraction in the composites was increased from 0 to 75 vol%, the CTEs of the composites increased from -9.1×10^{-6} to $-3.1 \times 10^{-6}\,K^{-1}$ and from -5.0×10^{-6} to $-1.9 \times 10^{-6}\,K^{-1}$ over the temperature ranges of 323–373 and 473–673 K, respectively. In composites with $Zr_2WP_2O_{12}$ volume fractions of 0–25 vol%, the experimentally obtained CTE values were in good agreement with the calculated values obtained by assuming mixed law behavior.

Acknowledgement

We thank KCM Corporation for providing the $Zr_2WP_2O_{12}$ powder samples.

References

1. Mary TA, Evans JSO, Vogt T, Sleight AW. Negative thermal expansion from 0.3 to 1050 Kelvin in ZrW_2O_8. *Science* 1996;**272**:90–2.
2. Evans JSO, Mary TA, Vogt T, Subramanian MA, Sleight AW. Negative thermal expansion in ZrW_2O_8 and HfW_2O_8. *Chem Mater* 1996;**8**: 2809–23.
3. Niwa E, Wakamiko S, Ichikawa T, Wang S, Hashimoto T, Takahashi K, et al. Preparation of dense ZrO_2/ZrW_2O_8 cosintered ceramics with controlled thermal expansion coefficients. *J Ceram Soc Jpn* 2004;**112**: 271–5.
4. Lommens P, De Meyer C, Bruneel E, De Buysser K, Van Driessche I, Hoste S. Synthesis and thermal expansion of ZrO_2/ZrW_2O_8 composites. *J Eur Ceram Soc* 2005;**5**:3605–10.
5. Yang X, Cheng X, Yan X, Yang J, Fu T, Qiu J. Synthesis of ZrO_2/ZrW_2O_8 composites with low thermal expansion. *Comp Sci Technol* 2007;**67**:1167–71.
6. Nishiyama S, Yoshida H, Hattori T.*Annu. Meet. Ceram. Soc.*. 2002. p. 1205.
7. Kanamori K, Kineri T, Fukuda R, Kawano T, Nishio K. Low-temperature sintering of ZrW_2O_8–SiO_2 by spark plasma sintering. *J Mater Sci* 2009;**44**:855–60.
8. Isobe T, Kato Y, Mizutani M, Ota T, Daimon K. Pressureless sintering of negative thermal expansion $ZrW_2O_8/Zr_2WP_2O_{12}$ composites. *Mater Lett* 2008;**62**:3913–5.
9. Tani J, Takahashi M, Kido H. Fabrication and thermal expansion of glass/ZrW_2O_8 composites. *Kagaku-to-Kogyo (Osaka)* 2008;**82**: 436–41.
10. Verdon C, Dunand DC. High-temperature reactivity in the ZrW_2O_8–Cu system. *Scripta Mater* 1997;**36**:1075–80.
11. Holzer H, Dunand DC. Phase transformation and thermal expansion of Cu/ZrW_2O_8 metal matrix composites. *J Mater Res* 1999;**14**:780–9.
12. Yilmaz S, Dunand DC. Finite-element analysis of thermal expansion and thermal mismatch stresses in a Cu–60 vol%ZrW_2O_8 composite. *Comp Sci Technol* 2004;**64**:1895–8.
13. Matsumoto A, Kobayashi K, Nishio T, Ozaki K. Fabrication and thermal expansion of Al–ZrW_2O_8 composites by pulse current sintering process. *Mater Sci Forum* 2003;**426–432**:2279–84.
14. Shi JD, Pu ZJ, Wu K-H, Larkins G. Composite materials with adjustable thermal expansion for electronic applications. *Mater Res Soc Symp Proc* 1997;**445**:229–34.
15. Sullivan LM, Lukehart CM. Zirconium tungstate (ZrW_2O_8)/polyimide nanocomposites exhibiting reduced coefficient of thermal expansion. *Chem Mater* 2005;**17**:2136–41.
16. Tani J, Kimura H, Hirota K, Kido H. Thermal expansion and mechanical properties of phenolic resin/ZrW_2O_8 composites. *J Appl Polym Sci* 2007;**106**:3343–7.
17. Evans JSO, Hu Z, Jorgensen JD, Argyriou DN, Short S, Sleight AW. Compressibility, phase transitions, and oxygen migration in zirconium tungstate, ZrW_2O_8. *Science* 1997;**275**:61–5.
18. Evans JSO, Mary TA, Sleight AW. Negative Thermal expansion in a large molybdate and tungstate family. *J Sol Stat Chem* 1997;**133**: 580–3.
19. Mary TA, Sleight AW. Bulk thermal expansion for tungstate and molybdates of the type $A_2M_3O_{12}$. *J Mater Res* 1999;**14**:912–5.
20. Martinek CA, Hummel FA. Subsolidus equilibria in the system ZrO_2–WO_3–P_2O_5. *J Am Ceram Soc* 1970;**53**:159–61.

21. Orrhede M, Tolani R, Salama K. Elastic constants and thermal expansion of aluminum–SiC metal–matrix composites. *Res Nondestr Eval* 1996;**8**:23–37.
22. Watanabe H, Tani J, Kido H, Mizuuchi K. Thermal expansion and mechanical properties of pure magnesium containing zirconium tungsten phosphate particles with negative thermal expansion. *Mater Sci Eng A* 2008;**494**:291–8.
23. *$Zr_2(WO_4)(PO_4)_2$ (ZWP) powder properties sheet*, KCM Corporation, Nagoya, Japan.
24. Balch DK, Fitzgerald TJ, Michaud VJ, Mortensen A, Shen Y-L, Suresh S. Thermal expansion of metals reinforced with ceramic particles and microcellular foams. *Metall Mater Trans A* 1996;**27A**:3700–17.